American Psychological Association

Journal of Experimental Psychology:
Learning, Memory, and Cognition

0278-7393/19/$12.00

2019, Vol. 45, No. 3, 497–514
http://dx.doi.org/10.1037/xlm0000597

Learning-Dependent Evolution of Spatial Representations in Large-Scale Virtual Environments

Michael J. Starrett, Jared D. Stokes, Derek J. Huffman, Emilio Ferrer, and Arne D. Ekstrom
University of California, Davis

An important question regards how we use environmental boundaries to anchor spatial representations during navigation. Behavioral and neurophysiological models appear to provide conflicting predictions, and this question has been difficult to answer because of technical challenges with testing navigation in novel, large-scale, realistic spatial environments. We conducted an experiment in which participants freely ambulated on an omnidirectional treadmill while viewing novel, town-sized environments in virtual reality on a head-mounted display. Participants performed interspersed judgments of relative direction (JRD) to assay their spatial knowledge and to determine when during learning they employed environmental boundaries to anchor their spatial representations. We designed JRD questions that assayed directions aligned and misaligned with the axes of the surrounding rectangular boundaries and employed structural equation modeling to better understand the learning-dependent dynamics for aligned versus misaligned pointing. Pointing accuracy showed no initial directional bias to boundaries, although such "alignment effects" did emerge after the fourth block of learning. Preexposure to a map in Experiment 2 led to similar overall findings. A control experiment in which participants studied a map but did not navigate the environment, however, demonstrated alignment effects after a brief, initial learning experience. Our results help to bridge the gap between neurophysiological models of location-specific firing in rodents and human behavioral models of spatial navigation by emphasizing the experience-dependent accumulation of route-specific knowledge. In particular, our results suggest that the use of spatial boundaries as an organizing schema during navigation of large-scale space occurs in an experience-dependent fashion.

Keywords: spatial cognition, navigation, learning, memory, virtual reality

Supplemental materials: http://dx.doi.org/10.1037/xlm0000597.supp

Representations of spatial information from our surrounding environment are critical for accomplishing everyday cognitive operations, such as navigating our neighborhood or an unfamiliar town we are visiting, yet what factors influence how we encode and retrieve this information remains debated. During navigation, the human brain receives optic flow from the visual system as well as body-based cues, including head-direction representations from the vestibular system and proprioceptive and somatosensory input regarding gait and other aspects of movement. Previous studies of human learning and memory in large-scale (town-sized) environments have utilized desktop-computer-based virtual reality (VR) interfaces comprised of a visual display monitor and joystick or controller (Chan, Baumann, Bellgrove, & Mattingley, 2013; Zhang, Zherdeva, & Ekstrom, 2014). A growing body of literature, however, suggests that such "desktop VR" interfaces may not accurately emulate real-world experiences because of a lack of vestibular information or, more importantly, proprioceptive information (Chrastil & Warren, 2012, 2013, 2014; Ruddle & Lessels,

This article was published Online First July 9, 2018.

Michael J. Starrett and Jared D. Stokes, Center for Neuroscience and Department of Psychology, University of California, Davis; Derek J. Huffman, Center for Neuroscience, University of California, Davis; Emilio Ferrer, Department of Psychology, University of California, Davis; Arne D. Ekstrom, Center for Neuroscience, Department of Psychology, and Neuroscience Graduate Group, University of California, Davis.

This research was supported by National Science Foundation BCS-1630296 and the University of California, Davis Chancellor's Award. Data and narrative interpretations from this research have been disseminated previously the following conferences: Annual Meeting of the Society for Neuroscience (November 2016), Spatial Cognition (August 2016), the Annual Meeting of the Cognitive Science Association for Interdisciplinary Learning (August 2017), and various internal academic and outreach presentations at the University of California, Davis. Michael J. Starrett and Arne D. Ekstrom designed the study. Michael J. Starrett and Jared D. Stokes, programmed the tasks. Michael J. Starrett performed data collection. Data analysis and interpretation was performed by Michael J. Starrett with help from Jared D. Stokes and under the supervision of Arne D. Ekstrom. Emilio Ferrer assisted with structural equation modeling analyses. Michael J. Starrett drafted the manuscript; Jared D. Stokes, Derek J. Huffman, Emilio Ferrer, and Arne D. Ekstrom provided critical revisions. All authors approved the final version of the manuscript for submission. We thank Patrick Cooke and Elijah Ziskin for assistance in data collection, and Branden Kolarik for helpful discussions. We also thank Oliver Kreylos for assisting in the acquisition of the omnidirectional treadmill.

Correspondence concerning this article should be addressed to Michael J. Starrett, Department of Psychology, University of California, Davis, One Shields Avenue, Davis, CA 95616. E-mail: mjstarrett@gmail.com

2006, 2009; Ruddle, Payne, & Jones, 1999; Taube, Valerio, & Yoder, 2013; Waller, Hunt, & Knapp, 1998). Thus, exactly how we form spatial representations in novel, large-scale spatial environments during free navigation, which involves using body-based cues, remains unclear. To address these issues in studying large-scale, city-sized virtual navigation, we used a novel, immersive VR interface that incorporates vestibular information via a head-mounted display (HMD) as well as proprioceptive and body-based rotational information via an omnidirectional treadmill.

One frequently reported finding from studies in small-scale spaces is that participants recall information faster and more accurately about relative locations of objects in an environment when aligned with its surrounding spatial geometry, termed *alignment effects*. Specifically, when participants are parallel to the axes of the boundaries of the room (e.g., a rectangle), they point to the relative positions of objects more accurately than when misaligned (Mou & McNamara, 2002; Rieser, 1989; Rump & McNamara, 2013; Shelton & McNamara, 2001). Thus, alignment effects appear to be a fundamental component of even nascent spatial representations and spatial memory (Waller, Montello, Richardson, & Hegarty, 2002). One important consideration when interpreting these results from small-scale "vista spaces," in which the entire layout is visible from one viewpoint, involves whether alignment effects would be present immediately in large-scale "environmental spaces," in which the geometric axes may not be as evident (Ekstrom & Isham, 2017; Meilinger, Strickrodt, & Bülthoff, 2016; Montello, 1993; Wolbers & Wiener, 2014).

Alignment effects are often thought to manifest based from two different components: relative to an observer's physical body position and rotation (i.e., to my right, left, front, or back), or based on imagined perspectives relative to the geometry, namely, the salient axes, of an environment. Mou, McNamara, Valiquette, and Rump (2004) showed that, in small-scale vista spaces, alignment effects were stronger when aligned not only with learning viewpoints but also when the body was oriented in the same direction as the proposed, imagined heading. Although this was observed even in circular rooms (i.e., no obvious primary axes), a later experiment showed that the bias for better performance when imagined and physical body headings were identical was abolished when testing occurred in a different, adjacent room (Kelly, Avraamides, & Loomis, 2007). That is to say, when testing occurred in the same room as learning, there was a benefit to being physically aligned with the salient axes of the room, whereas when testing occurred in a different room, participants performed equally well when physically aligned or misaligned with the salient axes of a geometrically identical, but novel, environment. Upon returning to the learning room, this "body-based" alignment benefit returned. Conversely, when participants were asked to always imagine themselves at the center of the testing room with the heading object directly in front of them, a "memory-based" alignment effect was present regardless of whether participants were tested in the same or a novel environment. This was interpreted as evidence for two forms alignment effects within a learned space: sensorimotor alignment effects, which are sensitive to body orientation, and memory alignment effects, which are sensitive to the salient geometry or primary axes of the learned environment, a distinction subsequently validated in numerous other studies (Kelly et al., 2007; Mou et al., 2004) and occur with conceptual changes in environment, based on verbal instructions, even in the absence of a physical room change (Shelton & Marchette, 2010). Such salient axes can be defined in environmental spaces by not only the geometry but even by streets (Werner & Schmidt, 1999) or landmarks (Marchette, Yerramsetti, Burns, & Shelton, 2011). Although both environmental (allocentric) and viewpoint-dependent (egocentric) information play a role in the formation of alignment effects, our focus in this particular study is on environmental (allocentric) alignment effects, given the theoretical interest in this topic in large-scale spaces, which we outline in more detail shortly.

Although there is compelling evidence that environmental alignment effects exist for both familiar (Frankenstein, Mohler, Bülthoff, & Meilinger, 2012; Werner & Schmidt, 1999) and recently learned (Iachini & Logie, 2003; McNamara, Rump, & Werner, 2003) large-scale spaces, these studies typically have not investigated alignment effects early in learning, in other words, after initial, brief exposure to an environment (e.g., walking around several blocks of an unfamiliar city only once). Specifically, these studies focused on assaying environmental alignment effects after participants had attained some criterion of familiarity within an environment, even if the criterion was low. However, it is also difficult to rule out that these participants may have had some exposure to the environment via maps or other sources that could have influenced their memory for the environmental boundaries. For example, Iachini and Logie (2003) showed alignment effects in college students who reported being totally or partially unfamiliar with the environment, although even the totally unfamiliar respondents had spent at least 1 and as many as 6 days in the environment. Indeed, even in the absence of any direct exposure, it is not uncommon to explore a map prior to visiting an unfamiliar university, city, park, etc. Thus, although there is clear evidence to support the notion that large-scale representations are, ultimately, not orientation-free, and that environmental alignment effects are detectable even in recently learned spaces, exactly when during exposure to a novel environment these alignment effects first manifest remains unaddressed.

Motivating their importance as a topic of further study, environmental alignment effects can be classified as a specific kind of mnemonic device for spatial cognition and memory, similar to "rules of thumb" such as estimating the sum of angles in a triangular spatial representation to be greater than the metrically true sum of 180° (Moar & Bower, 1983), biasing recall for spatial locations within a circle based on imagined vertical and horizontal (rather than diagonal) boundaries (Huttenlocher, Hedges, Corrigan, & Crawford, 2004), and believing that San Diego is West of Reno (it is not; Stevens & Coupe, 1978; for a recent review, see Ekstrom, Huffman, & Starrett, 2017). Identifying boundary conditions under which such mnemonic devices have weak or no effects on cognition until sufficient spatial information is encoded and integrated would provide a potential new line of study into the mechanisms underlying such cognitive phenomena and provide a better understanding of the integration of spatial information with environment-specific details (Ekstrom et al., 2017). The focus of the present research was thus specifically on environmental alignment effects in large-scale space, with VR affording the ability to more readily control testing intervals in large, realistic environments.

Under conditions in which environments are not immediately encoded with reference to evident geometric axes or by stereotyped, orthogonal paths, it is possible that there is a "critical period" for the

development and application of alignment effects for acquiring spatial knowledge, such as using the spatial boundaries to anchor one's representation of the environment. This would be consistent with human and rodent electrophysiological research into the neural substrates of spatial learning and memory showing that place cells often display little directional coding initially, particularly for unconstrained navigation in two-dimensional environments (Ekstrom et al., 2003; Markus et al., 1995; McNaughton, Barnes, & O'Keefe, 1983; Muller, Bostock, Taube, & Kubie, 1994; O'Keefe, 1976; M. A. Wilson & McNaughton, 1993). For constrained navigation (running on a track), however, directionality increases with repeated traversals of the same place fields during learning (Abbott & Blum, 1996; Ekstrom, Meltzer, McNaughton, & Barnes, 2001; Mehta, Barnes, & McNaughton, 1997; Mehta, Quirk, & Wilson, 2000). Indeed, place cells have been detailed during both encoding and retrieval of spatial and episodic memories (Miller et al., 2013), and may integrate information across learning and retrieval by interacting with head-direction, grid, and boundary vector cells (Taube et al., 2013). Thus, several studies in the place-cell literature, in contrast to behavioral findings on alignment effects, suggest that neural representations for space initially do not show direction dependence, but when they do, these may emerge as a function of experience (Abbott & Blum, 1996; Ekstrom et al., 2001; Mehta et al., 1997, 2000).

One issue when considering rodent studies of navigation is that it is challenging to port such findings to human behavior. and exactly how place cells manifest during the JRD task is unclear (although they are present during retrieval of spatial memories; e.g., Miller et al., 2013). Models of human spatial navigation and its neural underpinnings, however, would similarly predict a temporal dynamic in the emergence of alignment effects. Specifically, several models of human spatial cognition and navigation posit that a network of associated brain areas across the medial temporal lobe and parietal cortex may integrate information and translate between self- or viewpoint-based egocentric reference frames and allocentric reference frames, and vice versa (Byrne, Becker, & Burgess, 2007; Ekstrom et al., 2017; Epstein, 2008; Wang, 2017; Zhang & Ekstrom, 2013). These models also suggest the importance of temporal dynamics for the binding of spatial representations with aspects of the environment, such as the integrating of route-specific trajectories and the surrounding boundaries of the environment (e.g., egocentric to allocentric translation).

The goal of the present research, therefore, was to behaviorally identify a temporal window in which participants first employ spatial boundaries for encoding and retrieval of spatial representations during navigation of a novel, large-scale environment. Employing an omnidirectional treadmill coupled with an HMD was particularly advantageous because it allowed us to track body position and head direction in detail while continuously interspersing the JRD task during navigation. Three experiments investigated environmental alignment effects for spatial representations of such an environment by assessing spatial memory during repeated learning using judgments of relative direction (JRDs), in which participants inferred the location of a target based on an imagined heading comprised of two other landmark targets ("Imaging standing at A, facing B; point to C"). Each experiment varied the modality of learning, as route and map learning have been shown to have differential learning effects on spatial representations and the JRD task specifically (Thorndyke & Hayes-Roth, 1982; Zhang et al., 2014).

In Experiment 1, participants learned a virtual environment (VE) by freely navigating. In Experiment 2, initial navigation was preceded by map learning. In Experiment 3, participants learned using only maps. Consistent with the idea that navigation involves a dynamic integration of route-specific information with environmental geometry (like the environmental boundaries) during navigation, we hypothesized that alignment effects would not be present initially but would emerge after several learning experiences. This would support the idea that in large, complex environments like those that humans must learn and navigate daily, salient geometric axes must be integrated into evolving spatial representations. Alternatively, if alignment effects are present initially, it may be that they are employed very early on in the processing and integration of spatial information and thus are fundamental to representation of space. Here, we employed structural equation modeling (SEM), specifically, latent growth curve (LGC) modeling, because it allows us to deal with potential violations of the assumptions in an analysis of variance (ANOVA) when comparing learning curves and provides a principled method for comparing models involving a change in slope (i.e., no immediate alignment effects) versus a change in intercept (immediate alignment effects; Ferrer, Hamagami, & McArdle, 2004; Ferrer & McArdle, 2003; Jöreskog, 1971; Judd, McClelland, & Culhane, 1995; McArdle, 2009; West, Taylor, & Wu, 2012). Nonetheless, we report the results of analyses with conventional ANOVAs in the online supplemental materials, which are nonetheless consistent with our overall findings.

Experiment 1

We hypothesized that alignment effects would be weak or not detectible on the first block but would emerge later, after repeated learning. Alternatively, if alignment effects are an obligatory aspect of encoding a spatial representation during navigation, we might expect its emergence on the very first block. To test these ideas, we employed repeated navigation with interspersed pointing on the JRD task. Participants freely navigated a large-scale VR environment with an HMD on an omnidirectional treadmill; following one round of deliveries to each of the eight different stores in the environment, participants performed the JRD task for aligned and misaligned headings. We then repeated this navigation-JRD pointing procedure to determine when alignment effects might first emerge.

Method

Participants. We determined, based on previous research on the effects of spatial geometry on pointing accuracy in large-scale space using 24 participants (McNamara et al., 2003), that approximately such a sample size would be adequate to detect environment alignment effects using the JRD task. We note that subsequent studies have replicated this same basic finding of environmental alignment effects using comparable or smaller sample sizes (e.g., Mou & McNamara, 2002; Rieser, 1989; Rump & McNamara, 2013). A total of 43 participants were recruited from the University of California, Davis and the surrounding community. Each participant provided written informed consent prior to any study procedures, all of which were approved by the University of California, Davis Institutional Review Board. Participants were either paid or received extra credit in a psychology course. The experimenter withdrew two participants who

did not fit in the treadmill, four because of computer issues, one who did not meet inclusion criteria, 12 because of VR sickness, and one who failed to perform better than chance as assessed via a permutation test (for more information, see the section on data analyses). Data from 23 participants (nine female) with a mean age of 22.87 years were used in subsequent analyses.

Materials. The environment (Figure 1a) and experimental tasks (see Figure 2) were built in Unity 3D (Unity Technologies ApS, San Francisco, CA) using a modified version of the Landmarks v1.0 asset pack (developed by our laboratory in conjunction with BrickOvenGames; http://humanspatialcognitionlab.org/software/). The VE was approximately 226.71 × 309.01 m in size. In addition to various buildings and streets, the environment contained eight unique shops, which were the targets for navigation and the basis for the JRD questions.

Stimuli were viewed through an Oculus DK2 HMD (Oculus VR LLC, Menlo Park, CA) at a resolution of 960 × 1080 pixels per eye, 75 Hz refresh rate, and 100° (nominal) field of view. The tasks were run on an ABS Commander (ABS Computer Technologies Inc., Industry, CA) with an NVIDIA GeForce GTX 970 graphics card (NVIDIA Corp., Santa Clara, CA). Participants used a Cyberith Virtualizer omnidirectional treadmill (Cyberith GmbH, Herzogenburg, Austria) as the controller of their movement, with head turns rendered through the HMD (Figure 1b and Supplemental Video S1 in the online supplemental materials).

Procedure. Each participant received instructions and practiced until walking proficiently on the treadmill prior to testing (for more information, see the online Supplemental Methods section). Participants completed six alternating blocks of a navigation task (Figure 2a) and the JRD pointing task (Figure 2b). The resulting design was fully counterbalanced within subjects, resulting in a repeated measures design with 12 conditions, one for each alignment condition (aligned, misaligned) across each encoding/retrieval cycle (Block 1 through Block 6).

Navigation task. Participants were familiarized with the targets by viewing each of the target stores in a random order (repeated twice) and saying the names aloud prior to beginning the experiment. Participants then began each navigation block from one of six randomized starting locations. Each trial began with text indicating a navigation goal (10 s; Figure 2a, upper). Participants freely navigated the environment until the target store was found (Figure 2a, lower). This procedure was repeated for each store in a randomized order. After arriving at the final goal, JRD task instructions were presented.

JRD pointing task. Participants were given an Xbox 360 wireless controller (Microsoft Corporation, Redmond, WA) to respond to JRD questions. Questions were presented in the upper half of the display ("Imagine standing in Store A, facing Store B; point to Store C"). Participants rotated a virtual compass arrow clockwise (right trigger) or counterclockwise (left trigger) and submitted their response via a button press when they were confident in their pointing angle. There was no time limit, so if participants were unsure, they were required to guess. Participants were told to prioritize accuracy over speed. On each block, participants completed 28 JRD trials, half of which, randomly, were aligned parallel with the rectangular boundaries of the environment (aligned) and half of which were not (misaligned). Thus, we operationalized "aligned" to indicate headings of 0°, 90°, 180°, and 270° relative to the primary axes of the environmental boundaries. Consistent with past approaches (e.g., McNamara et al., 2003), all other headings were considered misaligned. After each block, participants were prompted to remove the HMD and take a short break. Example trials for the misaligned and aligned trials are shown in Figure 2b, and illustrations are shown overlaid on the VE in Figure 1a.

Data analyses. Data processing and analyses were completed in MATLAB 2016a (MathWorks Inc., Natick, MA) and RStudio (R Development Core Team, 2016; RStudio Team, 2015). Structural equation modeling analyses were conducted using Mplus (Version 8 Demo; Muthén & Muthén, 1998–2010).

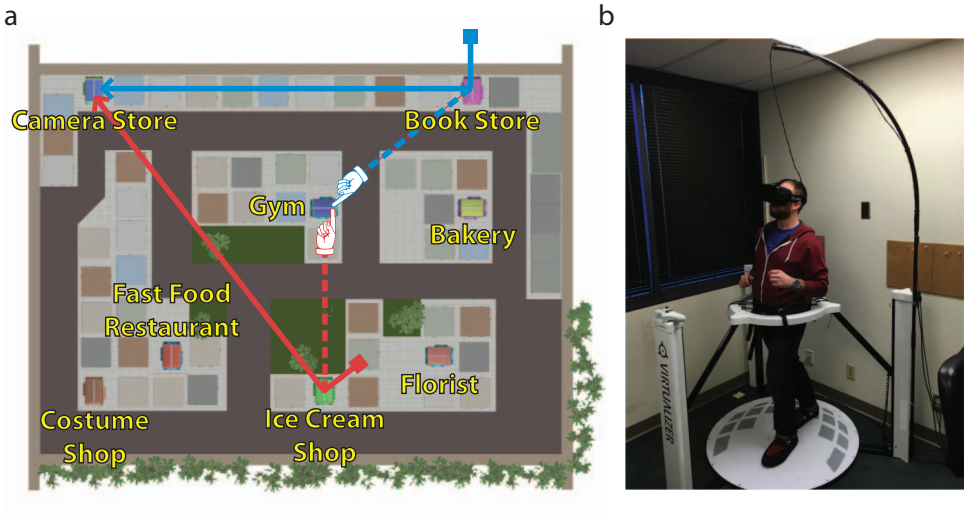

Figure 1. Aerial view of the virtual environment (VE) with (a) metric illustrations of misaligned trials (red [darker] lines) and aligned trials (blue [lighter] lines), and (b) the virtual reality interface, comprised of a head-mounted display worn by the user and an omnidirectional treadmill. The low-friction surface of the treadmill allowed participants to ambulate while remaining in place during navigating of the VE, which was much larger than the testing space. See the online article for the color version of this figure.

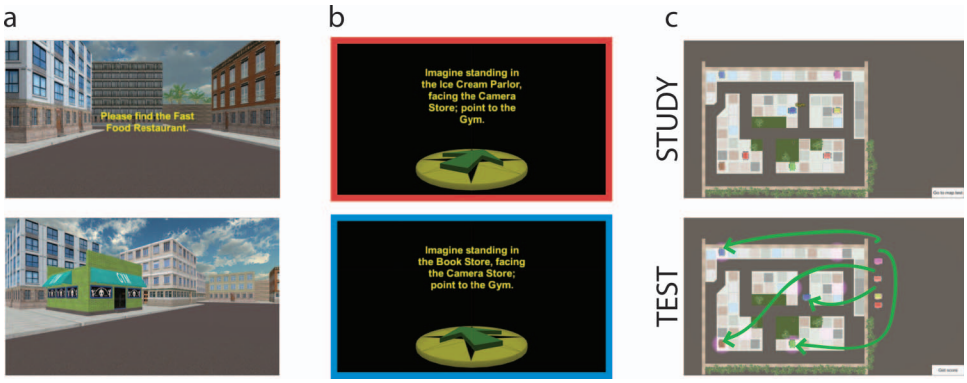

Figure 2. Route-learning task showing (a) a first-person viewpoint of an example trial goal instruction (top) and prospective target (bottom) for navigation; (b) judgment of relative directions task illustrating example misaligned and aligned questions with red (darker) and blue (lighter) borders, respectively, as in Figure 1; and (c) map-learning task showing the study phase (upper), in which the cursor is positioned above the "Gym," causing the text to appear, and the test phase (lower), showing hypothetical cursor movements to drop stores onto the map. See the online article for the color version of this figure.

Permutation tests. Participants whose average performance on the JRD task was not significantly better than chance, based on a permutation test that accounted for potential biases in both the initial position of the compass arrow (zero degrees/forward) and the distribution of the answers (i.e., not drawn from a uniform distribution around the compass) in the JRD task, were excluded from analyses (Huffman & Ekstrom, 2018; Huffman & Stark, 2017). Briefly, within each participant, the vector of responses was randomly shuffled and the median error was calculated. This procedure was repeated 10,000 times to generate a subject-specific null distribution. Participants were excluded if their empirical error was not in the lower 5% of the resultant null distribution (i.e., a one-tailed test). Note that this only resulted in one participant excluded for Experiment 1 and none for Experiment 2; we address this issue in more depth for Experiment 3.

Outlier trials. Responses of zero degrees (i.e., the compass arrow was not rotated before inputting a response) were excluded from further analyses. Given that the compass always started at or reset to zero (directly forward) and no pointing target was ever located directly in front of the imagined heading, these were treated as accidental button presses, resulting in only 11 of the total trials across all participants (0.27%) being removed. In subsequent Experiments, a 3-s delay was implemented on each trial before subjects could submit their JRD response, and as a result, there were no such trials in Experiment 2 or Experiment 3, supporting the idea that these trials were likely a result of accidental button presses. Additionally, mean performance across all trials and participants was calculated for each block. Trials greater than two standard deviations from the grand mean pointing error on each block (across trials and participants) were excluded as outliers, similar to Zhang et al. (2014).

LGC modeling. Because we expected that performance across learning blocks would not follow a linear trajectory, potentially violating assumptions of sphericity and homogeneity important to ANOVAs, we employed LGC models in structural equation modeling to better characterize the shape of aligned versus misaligned learning curves. Standard general linear modeling analysis techniques may also lack the power to detect effects such as the hypothesized interaction between aligned and misaligned performance, particularly when one of the factors has more than two levels (Judd et al., 1995), such as the block factor in our experiment. Using LGC models within the SEM framework thus provides additional power to detect these intergroup (for LGC modeling, we operationalize group[s] to refer to the within-subject conditions of alignment: aligned and misaligned) dynamics because of the ability to compare models with various parameters fixed to be equal or free to vary based on the hypothesized relationships between variables (McArdle, 2009). Nonetheless, results using ANOVA are included in the online supplemental materials, with the caveat that these will be sensitive to violations of linearity assumptions, an issue when looking for differences as a function of learning (i.e., an interaction effect).

The LGC model in our analyses is shown in Figure 3. The model included latent factors representing an intercept and a slope (represented as "*i*" and "*s*," respectively, in Figure 3), as well as variance components for each factor and their covariance (double-headed arrows in Figure 3). Performance for each block ($Y_{[n]}$ denoting mean performance on the nth block) loaded on both latent factors (the regressions for these factor loadings are represented by single-headed arrows in Figure 3). The intercept factor loadings were fixed, and the slope factor loadings were estimated. In particular, a latent growth model was employed in order to estimate a model with the best-fitting trajectory to the data, consistent with past approach using LGC (Ferrer & McArdle, 2003; West et al., 2012). For this, we fixed the factor loadings for the first and last block to 0 and –1, respectively, to represent the total change across learning. The remaining slope loadings—for Blocks 2 through 5—were estimated by the model, allowing for nonlinear change (Ferrer et al., 2004). Given that error variability was expected to decrease across learning, the model residuals ($e_{[n]}$ with double-headed arrow denoting the residual variance on the nth block that was not explained by the model; Figure 3) were allowed to differ for each block.

To evaluate differences in the model among the various alignment conditions, we used a multigroup approach (note the identically structured models in Figure 3 representing the aligned/mis-

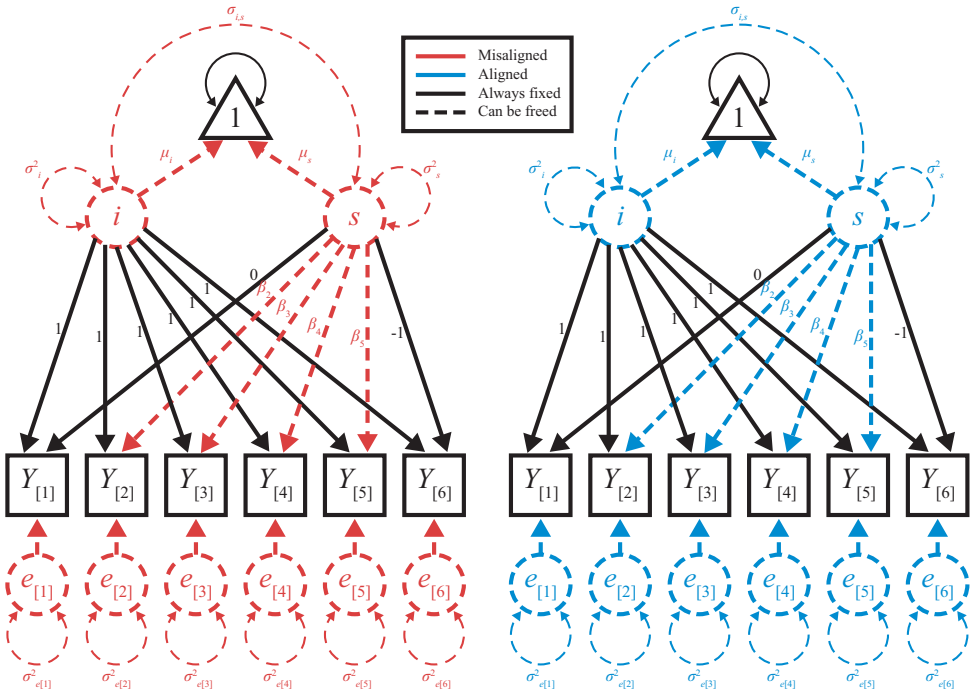

Figure 3. Path diagrams for structural equation models and manipulations of factorial invariance. The models for the misaligned (left, darker) and aligned (right, lighter) groups are identical in structure, but some parameters always remained fixed across the two group models, whereas others were systematically freed to vary, either individually or with other parameters based on theoretical hypotheses. Triangles represent constants, circles represent latent variables (i for intercept, s for slope, and e for residuals), and squares represent manifest variables (i.e., Y[3] on either side represents average pointing error for the third block of that condition group). Single-headed arrows indicate factor loadings/regression, and double-headed arrows indicate variance/covariance. See the online article for the color version of this figure.

aligned comparison). Here, an initial model was tested in which all parameters for the two groups were fixed to be invariant (i.e., complete factorial invariance). This is to indicate that the initial model assumes that performance in aligned and misaligned conditions is identical across all six blocks of testing. Next, various parameters were freed to vary between model groups to identify the model that best illustrates differences between the model groups (Jöreskog, 1971). First, based on hypothesized outcomes and possible alternatives, factorial invariance was relaxed across model groups for the slope mean, the intercept mean, or both. Subsequently, the covariance structure of the latent variables, shape of the curves across model groups as indicated by the slope loadings for Blocks 2 through 5, and the residuals were freed between model groups. The models for each group and the relaxation of factorial invariance constraints described in the LGC modeling section of the Experiment 1 methods are illustrated in Figure 3. To evaluate model fit and determine the most parsimonious model explaining the data, consistent with past approaches that have also done so, we used several fit indices including the chi square (χ^2), Akaike information criterion (AIC), Bayesian information criterion (BIC), comparative fit index (CFI), and root mean square error of approximation (RMSEA) to select the best-fitting model (West et al., 2012).

To quantify evidence in favor of the potential initial absence of alignment effects, JZS Bayes factors (BFs) were calculated for the misaligned–aligned pointing errors on the first block of each experiment (Rouder, Speckman, Sun, Morey, & Iverson, 2009) using the BayesFactors package for MATLAB (https://sampendu.wordpress.com/bayes-factors/). This test serves to provide information about the relative probability of obtaining the data under the null hypothesis (no alignment effects) as opposed to the alternative hypothesis (alignment effects present; i.e., how many times more likely were the data to be obtained under the null relative to the alternative?).

Comparison of absolute pointing error for each aligned versus misaligned block. Performance on the JRD task was quantified by absolute (unsigned) pointing error, calculated as the absolute value of the difference between the actual angle between heading and pointing vectors and the participant's estimate of that angle. To evaluate the specific emergence, or point at which alignment effects could be detected, *t* tests were conducted separately on each of the six blocks to compare misaligned and aligned absolute pointing error. We additionally checked to see whether performance was significantly better for a single arbitrarily defined cardinal direction (North, East, South, West) based on the primary axes of the environment (Gagnon et al., 2014). Although informative, the cardinal direction comparisons should be interpreted with some caution, as there were a somewhat limited number of the 14 aligned trials on each block that were facing each cardinal direction.

Additional analyses. Details for additional analyses, including JRD response latency, excess navigation path length, and head

direction during navigation are provided in the online supplemental materials.

Results

Latent growth curve modeling. A total of 5.90% of trials were excluded from further analyses as outliers or accidental button presses, as described in the Data Analysis in the Method section. Of the models tested, the model in which only the latent slope means were free to differ between model groups was selected as the best predictor of the actual data (shown as dotted lines in Figure 4a). The path diagram for the selected "slope mean" model is shown in Figure 4b. As shown in Figure 4a, the model predicts actual performance quite well (solid and dotted lines for actual data and model predictions, respectively), and predicted outcomes on the first block fall within the confidence intervals of the aligned and misaligned errors. Both the data and model also clearly show a difference in overall change between model groups. Fit indices for all models tested are shown in Table 1. The selected model fit significantly better than the complete invariance model, $\chi^2_{diff}(1) = 12.64$, $p < .001$. The next step in relaxing factorial invariance, freeing both the latent slope mean and the latent intercept mean, did not significantly improve LGC model fit, $\chi^2_{diff}(1) = 0.04$, $p > .250$; therefore, further difference tests on more saturated models were not conducted. The "intercept mean" model with the same degrees of freedom as the "slope mean" model also fit significantly better than the complete invariance model, $\chi^2_{diff}(1) = 11.68$, $p = .001$. Consistent with past approaches, we thus selected the "slope mean" model over the "intercept mean" model, as it performed numerically better (see Table 1) across all calculated fit indices (West et al., 2012). This model predicted the absence of an alignment effect on the first block (Figure 4a, dotted lines), meaning that aligned and misaligned performance will be equivalent on the first block, but the total average improvement in pointing performance across learning will be greater for aligned trials. Given that this experiment was designed explicitly to detect early changes in the presence and strength of alignment effects, the "slope mean" model provided predictions that were compatible with hypothesized dynamics of alignment effects (Ferrer & McArdle, 2003). The BF calculated for the difference scores for Block 1 also weakly suggested that these results were most likely obtained under the hypothesis that there was no misaligned–aligned difference in pointing error ($BF_{01} = 1.60$). Although not definitive, this result is in agreement with the selected model for predicting the data in which overall change is different but initial performance on misaligned and aligned trials is equal.

Comparison of absolute pointing error for each aligned versus misaligned block. Based on our a priori hypotheses, two-tailed paired *t* tests were conducted to evaluate differences in

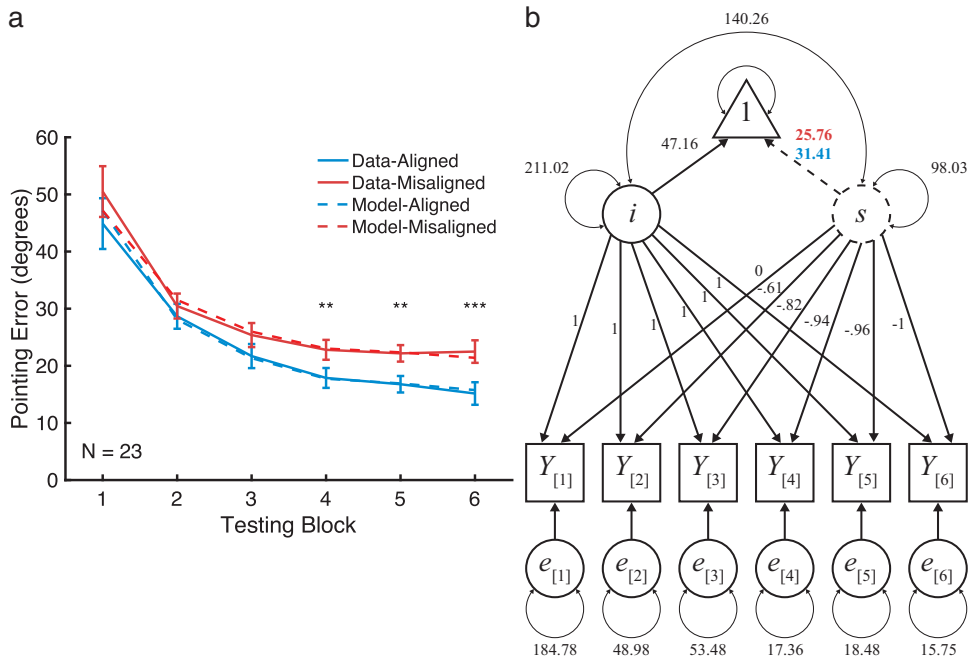

Figure 4. Experiment 1 (a) performance on the judgment of relative directions in each alignment condition for each block (solid lines) and model predictions for these same data (dotted lines), based on the selected latent growth modeling model as well as (b) the path diagram for the selected model, including all estimated parameters, both fixed (solid lines) and freed (dotted lines). Error bars represent 95% confidence intervals that have been visually adjusted to remove between-subjects variability (Cousineau, 2005). For model parameters freed across groups, misaligned parameter estimates are shown in red (dark gray) and aligned parameters estimates are shown in blue (light gray). Asterisks indicate significant differences between misaligned and aligned conditions on a given block. * $p < .05$. ** $p < .01$. *** $p < .001$. See the online article for the color version of this figure.

Table 1
Models Tested and Corresponding Fit Indices for Experiment 1

Parameter(s) free	χ^2	*df*	*p*	AIC	BIC	CFI	RMSEA
Complete invariance	49.87	39	.114	1,933.39	1,960.82	.921	.110
Slope mean	**37.23**	**38**	**.505**	**1,922.75**	**1,952.00**	**1**	**0**
Intercept mean	38.19	38	.461	1,923.71	1,952.97	.999	.015
Slope and intercept mean	37.19	37	.461	1,924.70	1,955.79	.999	.015
Variance/covariance	36.49	34	.354	1,930.00	1,966.58	.982	.056
Curvature (Betas 2–5)	29.89	30	.471	1,931.41	1,975.30	1	0
Residuals	22.97	24	.521	1,936.49	1,991.35	1	0

Note. Models are described in the left column in order of decreasing factorial invariance between the misaligned and aligned group models. Subsequent columns indicate the value for fit indices used for model selection. The bolded row indicates the selected model. *df* = degrees of freedom; AIC = Akaike information criterion; BIC = Bayesian information criterion; CFI = comparative fit index; RMSEA = root mean square error of approximation.

pointing error for misaligned versus aligned trials across each learning block. There were no significant differences between misaligned and aligned pointing on the first, second, or third block. Significant alignment effects emerged on the fourth retrieval block and were stable throughout the remaining blocks—Blocks 5 and 6. Descriptive statistics and comparisons for misaligned and aligned conditions across all six blocks are reported in Table 2. The increasing effect size and ability to detect statistically significant alignment effects only on later blocks lent further theoretical justification for a "slope mean" model to predict the data (Ferrer & McArdle, 2003). Group-averaged absolute pointing errors for misaligned and aligned conditions across learning are shown in Figure 4a. Wilcoxon's signed-rank sum tests revealed the same pattern in the response latency data, although we stress the untimed nature of our task and emphasis on accuracy over speed in the instructions. More information on latencies can be found in the online supplemental materials and online Figure S1. Performance was not significantly different between imagined headings facing in cardinal directions except for on the fourth block, in which headings facing South were significantly better than those facing North, although this difference did not exist on any other testing block. Performance for each cardinal-facing direction across testing blocks is shown in online Figure S7.

Additional analyses. The routes traveled during navigation (one representative participant's routes are shown for each block of navigation in online Figure S2) were used to calculate excess path traveled relative to the shortest possible distance from the start location to the target. Excess path consistently decreased over blocks, suggesting that participants navigated the routes more efficiency as a function of exposure (excess path analyses are detailed in the online supplemental material and Figure S3a). There was no correlation between the difference in misaligned and aligned pointing error and excess path length, suggesting that navigational accuracy was unrelated to aligned versus misaligned differences (Figure S4a). The proportion of time that participants spent orienting their head in various directions during navigation is shown in Figure S5a, and a comparison of cardinal (i.e., N, S, E, W) versus intercardinal (NE, SE, SW, NW) orienting time is

Table 2
Comparison of Aligned and Misaligned Pointing Conditions Across Retrieval Blocks in Experiment 1

Retrieval block	*M*	*SD*	M_{diff}	*df*	*t*	*p*	*d*	95% CI
Block 1								
Misaligned	50.5	20.24	5.61	22	1.56	.134	.32	[−1.87, 13.08]
Aligned	44.89	18.41						
Block 2								
Misaligned	30.46	10.39	1.79	22	1.06	>.250	.22	[−1.71, 5.30]
Aligned	28.67	12.99						
Block 3								
Misaligned	25.38	11.05	3.68	22	3.25	.093	.37	[−.66, 8.01]
Aligned	21.7	9.89						
Block 4								
Misaligned	22.8	6.46	4.93	22	3.25	.004	.68	[1.78, 8.06]
Aligned	17.87	8.13						
Block 5								
Misaligned	22.18	7.34	5.41	22	3.8	.001	.79	[2.46, 8.35]
Aligned	16.77	8.19						
Block 6								
Misaligned	22.49	6.39	7.34	22	6.5	<.001	1.36	[5.00, 9.68]
Aligned	15.15	5.79						

Note. *df* = degrees of freedom; CI = confidence interval.

shown in Figure S5b. Participants spent more time facing the cardinal directions starting on Block 1, suggesting that facing direction during navigation was not directly related to the emergence of alignment effects during the JRD task. There was no evidence that the initial or final head orientation on the navigation blocks had any effect on biasing the imagined headings in the JRD trials (Figure S6).

Discussion

Participants freely navigated a large-scale VE with vestibular, proprioceptive, and somatosensory information available. Consistent with our hypothesis, the best-fitting model for the data predicts no alignment effects initially, with these effects emerging later because of greater improvements on aligned pointing compared with misaligned. Specifically, for the best-fitting model, the only parameter that differed between aligned and misaligned trials in this analysis was the slope mean, suggesting that misaligned error decreased at a slower rate than aligned error. The difference in slope means, rather than intercept means, indicates that aligned and misaligned pointing errors are the same initially but diverge over time. These findings are bolstered by the Bayesian analysis and planned comparisons. Thus, the findings from Experiment 1 suggest that alignment effects are an experience-dependent phenomenon when exploring a novel spatial environment and do not emerge until approximately four blocks of exposure to a spatial environment.

One potential concern with these results was that the limited exposure prior to the first block of JRDs may have resulted in participants' absolute pointing error being too high or too variable to detect differences between aligned and misaligned conditions. In other words, on the first blocks of learning, when participants had the least knowledge about the environment, their pointing variability was likely highest (qualitatively shown in Figure 4a). This increased variability, in principle, could have accounted for the lack of any significant differences in Experiment 1. We reasoned that if participants were preexposed to a map of the environment, this would likely reduce their initial pointing error and variability, allowing us to evaluate the extent to which relatively worse performance on early JRD blocks may have prevented us from detecting alignment effects if they were in fact present in Block 1 of Experiment 1 but occluded by "noise" (i.e., Type II error). In addition, preexposure to a map would provide participants with knowledge of the shape of the environmental boundaries prior to exposure to the environment via navigation. Thus, based on the idea that alignment effects are an experience-dependent phenomenon, we might expect them to emerge earlier when participants are exposed to a map and navigation before initial testing.

Experiment 2

To test the effect of brief, prior exposure to the salient axes of the environment, participants completed a map-learning task prior to navigational learning. We hypothesized that this relatively low-effort prior map learning task would provide additional information that could elicit earlier alignment effects than in Experiment 1, while also reducing mean pointing error and variability on early blocks, which may also have affected the ability to detect alignment effects on these early JRD blocks in Experiment 1. Alternatively, if alignment effects are present after initial map and route learning, this would provide evidence for the importance of map learning in utilizing alignment effects, or at least suggest that the combination of map and route information is necessary to utilize the axes of the environment initially.

Method

Participants. A total of 43 participants, who had not participated in Experiment 1, were recruited following the same procedures as Experiment 1. The experimenter withdrew one participant because of fatigue, two because of computer issues, two who did not meet inclusion criteria, 13 because of VR sickness, and one who was unable to use the treadmill proficiently. Data from 24 participants (11 female; mean age = 22.13 years) were used for subsequent analyses.

Procedure. The procedure for Experiment 2 was identical to Experiment 1, with the addition of a map-learning task on an external computer monitor between training and the first navigation block (Figure 2c). This yielded an otherwise identical experimental design to Experiment 1.

In the map-learning task, participants were given unlimited time to study an aerial view of the VE and learn the names and locations of the eight stores (Figure 2c, "STUDY"). Participants learned store names and locations by moving the cursor over the top of a given store, at which point the name of the store was displayed in text adjacent to the store on the map. After participants were confident they knew the locations of all stores, they began the testing phase. For this phase, stores were moved from within the VE to outside the boundary wall of the VE, and participants had to drag and drop them in the correct location (Figure 2c, "TEST"). Participants repeated "study" and "test" until they reached criterion (100% correct). Note that they were already familiarized with the names and images of the stores prior to map learning, which they experienced during the familiarization phase (for a description, see Experiment 1).

Results

Latent growth curve modeling. In total, 5.93% of trials were excluded as outliers based on the same criteria used in Experiment 1. As in Experiment 1, the LGC results favored a model in which only the latent slope means were free to vary between aligned and misaligned model groups for predicting performance from Experiment 2 (Figure 5a, dotted lines), supporting the conclusion that alignment effects were not present on the first block (Figure 5b). Qualitatively, model predictions fit well with actual pointing error outcomes, and the discrepancy in overall change between aligned versus misaligned conditions is clear, even more so than in Experiment 1 (Figure 5a). The fit indices for all models tested are shown in Table 3. The selected model fit significantly better than the complete invariance model, $\chi^2_{diff}(1) = 22.08$, $p < .001$. The next step in relaxing factorial invariance, freeing both the latent slope mean and the latent intercept mean, did not significantly improve LGC model fit, $\chi^2_{diff}(1) = 0.01$, $p > .250$; therefore, further difference tests on more saturated models were not conducted. The "intercept mean" model with the same degrees of freedom as the "slope mean" model also fit significantly better than the complete invariance model, $\chi^2_{diff}(1) = 20.23$, $p < .001$. Again, we selected the "slope mean"

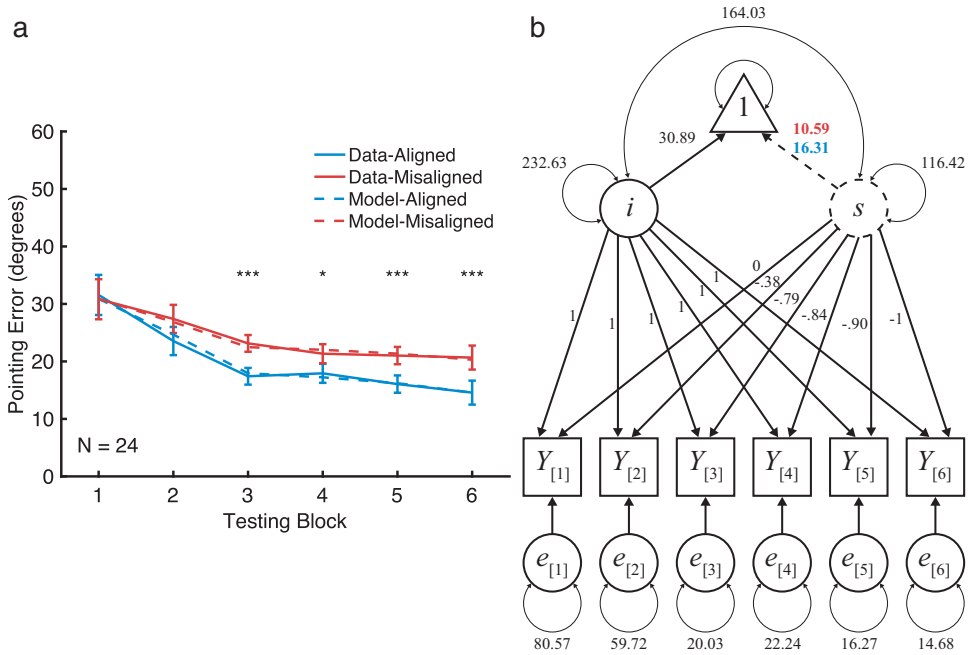

Figure 5. Experiment 2 (a) performance on the judgment of relative directions in each alignment condition for each block (solid lines) and model predictions for these same data (dotted lines), based on the selected latent growth modeling model as well as (b) the path diagram for the selected model, including all estimated parameters, both fixed (solid lines) and freed (dotted lines). Error bars represent 95% confidence intervals that have been visually adjusted to remove between-subjects variability (Cousineau, 2005). For model parameters freed across groups, misaligned parameter estimates are shown in red (dark gray) and aligned parameters estimates are shown in blue (light gray). Asterisks indicate significant differences between misaligned and aligned conditions on a given block. * $p < .05$. ** $p < .01$. *** $p < .001$. See the online article for the color version of this figure.

model, as it had numerically better fit indices on all calculated indices (see Table 3; Ferrer & McArdle, 2003; West et al., 2012). The BF for Block 1 misaligned–aligned pointing difference provided sufficient evidence that these data were more likely obtained under the null hypothesis ($BF_{01} = 4.47$). This is compatible with the LGC modeling results suggesting identical intercept means in the learning curves for performance aligned versus misaligned JRD trials, consistent with Experiment 1 but with additional evidence for the stronger likelihood of a null result on the first block using the ratio for the BF.

Comparison of absolute pointing error for each aligned versus misaligned block. Planned comparisons again revealed no alignment effects detected on the first or second block. Significant alignment effects were detected on all of the remaining blocks, Blocks 3 through 6. Descriptive statistics and comparisons for

Table 3
Models Tested and Corresponding Fit Indices for Experiment 2

Parameter(s) free	χ^2	*df*	*p*	AIC	BIC	CFI	RMSEA
Complete invariance	59.50	39	.019	1,958.84	1,986.90	.895	.148
Slope mean	**37.42**	**38**	**.496**	**1,938.75**	**1,968.69**	**1**	**0**
Intercept mean	39.27	38	.413	1,940.61	1,970.54	.994	.037
Slope and intercept mean	37.41	37	.450	1,940.75	1,972.56	.998	.022
Variance/covariance	34.79	34	.430	1,944.12	1,981.54	.996	.031
Curvature (Betas 2–5)	31.02	30	.414	1,948.36	1,993.26	.995	.038
Residuals	20.58	24	.663	1,949.92	2,006.05	1	0

Note. Models are described in the left column in order of decreasing factorial invariance between the misaligned and aligned group models. Subsequent columns indicate the value for fit indices used for model selection. The bolded row indicates the selected model. *df* = degrees of freedom; AIC = Akaike information criterion; BIC = Bayesian information criterion; CFI = comparative fit index; RMSEA = root mean square error of approximation.

misaligned and aligned conditions across all six blocks are reported in Table 4. Group-averaged absolute pointing errors for misaligned and aligned conditions across learning are shown in Figure 5a. The same overall pattern of alignment effects was also present in the response latency data (Figure S1 of the online supplemental materials). Performance was not significantly different between imagined headings facing "North" and any other headings in cardinal directions (Figure S7).

We compared the first block of JRD pointing in Experiment 1 with Experiment 2 to confirm that pointing error decreased as a result of map exposure. This was indeed the case. We entered the data from the first and second blocks of Experiments 1 and 2 into a 2 (experiment: 1, 2) × 2 (block: 1, 2) mixed ANOVA. By using only two time points (Blocks 1 and 2), this "restricted" data set should thus provide more reliable results from linear modeling approaches, like ANOVA, compared with using the entire data set that follows a nonlinear trajectory across blocks. There were main effects of experiment, $F(1, 45) = 6.48$, $p = .014$, and block, $F(1, 45) = 63.09$, $p < .001$, as well as a significant Experiment × Block interaction, $F(1, 45) = 17.45$, $p < .001$. These findings bolstered the idea that preexposure to the map significantly reduced pointing error in Experiment 2. A Welch's t test indicated overall error on the first block in Experiment 2 ($M = 31.19$, $SD = 17.41$) was significantly lower than in Experiment 1 ($M = 47.69$, $SD = 19.34$), $t(90.04) = 4.34$, $p < .001$, $d = 0.90$, 95% confidence interval [CI] [8.95, 24.05]. Pointing error, however, was not significantly lower on the second block in Experiment 2 ($M = 25.47$, $SD = 14.28$) compared with Experiment 1 ($M = 29.56$, $SD = 11.67$), $t(89.77) = 1.52$, $p > .250$, $d = 0.31$, 95% CI [−1.24, 9.43]. Although there was a significant improvement in performance across the first two blocks in Experiment 1, $t(73.93) = 5.44$, $p < .001$, $d = 1.14$, 95% CI [11.49, 24.76], this was not true for Experiment 2, $t(90.55) = 1.76$, $p > .250$, $d = 0.36$, 95% CI [−0.73, 12.18], evidenced by the interaction effect in the 2 × 2 ANOVA. The p values for these post hoc tests were Bonferroni corrected for multiple (four) comparisons. We also directly compared the degree of variability in pointing error on Blocks 1 and 2 using Bartlett's test to determine whether these differed as a function of blocks for Experiment 1 versus 2. Although there was a significant difference in variance for pointing error between the first and second block in Experiment 1 ($SD_1 = 17.48$, $SD_2 = 11.03$), $\chi^2_{diff}(1) = 4.41$, $p = .036$, this difference in variance was not significant in Experiment 2 ($SD_1 = 16.39$, $SD_2 = 13.48$), $\chi^2_{diff}(1) = 4.41$, $p > .250$. These additional analyses suggest that although there was greater variability in pointing error on the first block than on the second in Experiment 1, preexposure to a map in Experiment 2 resulted in more stable variability early in learning. Thus, it is unlikely that poor performance on early blocks of Experiment 1 prevented us from detecting actual alignment effects.

Additional analyses. Excess path results are shown in Figure S3b (in the online supplemental materials), again demonstrating improved route efficiency over navigation blocks, although excess path was lower on Block 1 in Experiment 2 than Experiment 1, consistent with the effects of preexposure to the map on JRD pointing error. The correlation between excess path and the difference between misaligned and aligned pointing difference again failed to reach significance (Figure S4b). Results from head orientation analyses for Experiment 2 are shown in Figures S5a, S5b, and S6; just as in Experiment 1, participants faced the cardinal directions more often than the noncardinal directions beginning on Block 1, again suggesting that facing direction during navigation could not directly account for the later emergence of alignment effects during the JRD task. Consistent with Experiment 1, initial and final heading during navigation did not account for variance in JRD pointing error.

Discussion

In Experiment 2, we exposed participants to the same learning procedure as Experiment 1, with the addition of prior map learning before navigation. Consistent with only navigation learning in Experiment 1, the LGC models for Experiment 2 data favored a

Table 4
Comparison of Aligned and Misaligned Pointing Conditions Across Retrieval Blocks in Experiment 2

Retrieval block	*M*	*SD*	M_{diff}	*df*	*t*	*p*	*d*	95% CI
Block 1								
Misaligned	30.82	14.52	−.74	23	−.3	>.250	−.06	[−5.88, 4.39]
Aligned	31.56	20.20						
Block 2								
Misaligned	27.39	14.29	3.84	23	1.82	.082	.37	[−.52, 8.21]
Aligned	23.55	14.32						
Block 3								
Misaligned	23.14	7.93	5.72	23	4.35	<.001	.89	[3.00, 8.45]
Aligned	17.42	8.66						
Block 4								
Misaligned	21.34	7.53	3.41	23	2.56	.018	.52	[.65, 6.17]
Aligned	17.93	8.12						
Block 5								
Misaligned	21.02	7.50	4.96	23	3.49	<.001	.80	[2.36, 7.56]
Aligned	16.06	7.10						
Block 6								
Misaligned	20.67	5.81	6.10	23	5.14	<.001	1.05	[3.64, 8.55]
Aligned	14.57	6.05						

Note. *df* = degrees of freedom; CI = confidence interval.

model predicting a different total change across learning, with misaligned pointing error decreasing less overall, as the only variable component of the model across groups. Again, the difference in slope means, rather than intercept means, suggests that aligned and misaligned pointing error started at the same level but diverged over time. As predicted, the additional information prior to the first retrieval block resulted in lower absolute pointing error, with participants performing better on the first retrieval block of Experiment 2 compared with Experiment 1. In Experiment 2, there was also no decrease in variance from the first to second block that would have added noise to the data and decreased the ability to detect alignment effects if they were present. Importantly in Experiment 2, although we did see alignment effects one block earlier, the difference between aligned and misaligned was not significant on the first or second block using *t* tests, further supported by the Bayes null finding of 4.47. These results further support a model by which alignment effects are not encoded initially, but rather manifest via underlying cognitive and neural mechanisms during repeated learning. To better understand the specific impact of cartographic knowledge on alignment effects and the interaction between studying a map versus route learning, we conducted a third experiment in which learning only occurred via maps.

Experiment 3

Participants in Experiment 3 learned the environment using the map task from Experiment 2 as the only form of learning across repeated experience. Thus, Experiment 3 served as the "aerial view" learning analog to the "first-person view" learning in Experiment 1, in which only route learning was employed. Based on Experiments 1 and 2 not showing initial alignment effects, we hypothesized that alignment effects would once again not manifest until after sufficient exposure, because participants in Experiment 2 had both map and navigation information available to be integrated for spatial memory. Alternatively, it is possible that route learning after map learning introduced retroactive interference on map-based spatial representations, which would instead suggest that direct perception of the environmental geometry via a cartographic map may facilitate the formation of alignment effects. If the latter is true, then we may see alignment effects as early as the first block when the interference of route information is removed. This would be consistent with the often-reported finding of alignment effects in small-scale spaces (Mou & McNamara, 2002; Rieser, 1989; Rump & McNamara, 2013; Shelton & McNamara, 2001).

Method

Participants. A total of 64 participants were recruited following the same procedures used in Experiments 1 and 2. One participant withdrew from the study. The experimenter withdrew four participants who did not finish in the allotted time, one who did not follow the task instructions, two because of computer errors, and nine that failed to perform significantly better than chance. Data from 47 participants (25 female; mean age = 20.93 years) were used for subsequent analyses. None of these participants had participated in the past experiments. The reasons for the differences in sample size are as follows: We collected an initial sample of 24 participants (see the online supplemental materials for more information on this subset of the final sample), finding significant alignment effects on all blocks *except* the second. Because of large qualitative difference between the *p* values for the *t* tests on the first two blocks and a failure for one of the tested LGC models to converge, we added an additional 23 subjects from a pilot study with an identical design to Experiment 3 to the initial sample and included them for further analysis (i.e., we approximately doubled the sample size). The results from the large ($n = 47$) and small ($n = 24$) samples are largely identical (see the online supplemental materials), and thus subsequent results are reported based on the larger sample that allowed us to run the LGC models. Note, again, that the smaller sample size, which was consistent with Experiments 1 and 2, yielded essentially identical results, with exception of the convergence of the LGC, and is described in detail in the online supplemental materials.

Procedure. The procedure for Experiment 3 was identical to Experiment 1, except that the map-learning task, completed on either a 21.5-in. or 27-in. iMac computer (Apple Inc., Cupertino, CA), replaced the navigation task on each block as the only modality for learning. The map task was identical to the one used in Experiment 2; the familiarization and JRD tasks were identical to the ones used in Experiments 1 and 2. This yielded a structurally identical experimental design to Experiments 1 and 2.

Results

Latent growth curve modeling. A total of 5.69% of trials were excluded as outliers from further analysis based on the same criteria as in previous experiments. The LGC model used in the first two experiments was modified to account for the fact that little to no change occurred after Block 2 in Experiment 3; otherwise, the models did not converge. Specifically, the slope factor loadings on Blocks 3 through 5, in addition to Block 6, were all fixed to negative one and the residuals for Blocks 3 through 6 were fixed to be equal, predicting no change in performance or variability after Block 2. Because most of the models contained a nonsignificant negative residual variance for the first block, this value was fixed to zero, which had no impact on model selection, while rectifying this issue in the variance-covariance matrix of the model. Compared with the models used in Experiments 1 and 2 (in which the curvature was estimated for each block), this model (in which curvature was only estimated on Block 2, with no change from Blocks 3 through 6) fit the data from Experiment 3 best. Modifications to the model are illustrated in Figure 6b. Across all models, only the model with the latent intercept free and the complete invariance model did not differ significantly from the observed data (all other ps $< .05$; see Table 5). Although the complete invariance model performed better on several fit indices (see Table 5), it estimated several additional parameters, which is reflected in the BIC index and the fact that it did not fit significantly better than the intercept-only model, $\chi^2_{diff}(7) = 11.38$, $p = .123$. Thus, the model best describing the data from Experiment 3 (Figure 6a, dotted lines) was one in which only the latent intercept means, and not the latent slope means, were free to vary between model groups. This model predicts that aligned and misaligned trials will be significantly different on the first block and will change identically over time. The BF for Block 1 misaligned–aligned pointing difference provided weak evidence that the data was obtained under the alternative hypothesis (i.e., a model in which an alignment effect exists on the first block),

Table 5
Models Tested and Corresponding Fit Indices for Experiment 3

Parameter(s) free	χ^2	*df*	*p*	AIC	BIC	CFI	RMSEA
Complete invariance	67.63	45	.016	3,939.86	3,962.75	.900	.103
Slope mean	61.33	44	.043	3,935.56	3,961.00	.924	.092
Intercept mean	**60.05**	**44**	**.054**	**3,934.28**	**3,959.71**	**.929**	**.088**
Slope and intercept mean	59.95	43	.045	3,936.18	3,964.15	.925	.092
Variance/covariance	59.69	40	.023	3,941.92	3,977.53	.913	.102
Curvature (Beta 2)	59.58	39	.019	3,943.81	3,981.96	.909	.106
Residuals	48.67	37	.095	3,936.90	3,980.14	.949	.082

Note. Models are described in the left column in order of decreasing factorial invariance between the misaligned and aligned group models. Subsequent columns indicate the value for fit indices used for model selection. The bolded row indicates the selected model. *df* = degrees of freedom; AIC = Akaike information criterion; BIC = Bayesian information criterion; CFI = comparative fit index; RMSEA = root mean square error of approximation.

$BF_{01} = 0.90$. This provides further support for the LGC results, as the BF is consistent with modeling results in all three experiments, including the likelihood favoring initial alignment effects here, in Experiment 3.

Comparison of absolute pointing error for each aligned versus misaligned block. Group-averaged absolute pointing errors for misaligned and aligned conditions across the six testing blocks are shown in Figure 6a. Planned comparisons revealed a significant difference between misaligned and aligned performance on Block 1. This effect was marginally significant for Block 2 and significant for the remaining blocks—Blocks 3 through 6. Descriptive statistics and comparisons for misaligned and aligned conditions across all six blocks are reported in Table 6.

For the first testing block, absolute pointing error for imagined headings facing North ($M = 20.10$, $SD = 17.55$) was significantly lower than for headings facing East ($M = 28.84$, $SD = 21.22$), $t(45) = -2.65$, $p = .034$, 95% CI [−14.71, −1.99], or West ($M = 27.84$, $SD = 19.94$), $t(45) = -2.89$, $p = .018$, 95% CI [−13.48, −2.42], but

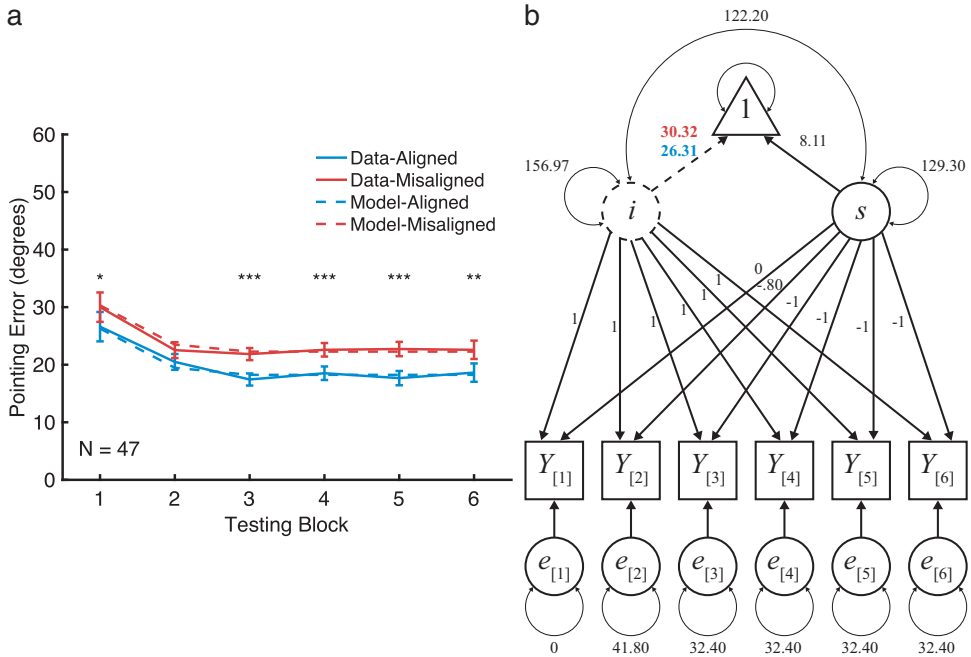

Figure 6. Experiment 3 (a) performance on the judgment of relative directions in each alignment condition for each block (solid lines) and model predictions for these same data (dotted lines), based on the selected latent growth modeling model as well as (b) the path diagram for the selected model, including all estimated parameters, both fixed (solid lines) and freed (dotted lines). Error bars represent 95% confidence intervals that have been visually adjusted to remove between-subjects variability (Cousineau, 2005). For model parameters freed across groups, misaligned parameter estimates are shown in red (dark gray) and aligned parameters estimates are shown in blue (light gray). Asterisks indicate significant differences between misaligned and aligned conditions on a given block. * $p < .05$. ** $p < .01$. *** $p < .001$. See the online article for the color version of this figure.

Table 6
Comparison of Aligned and Misaligned Pointing Conditions Across Retrieval Blocks in Experiment 3

Retrieval block	*M*	*SD*	M_{diff}	*df*	*t*	*p*	*d*	95% CI
Block 1								
Misaligned	30.00	12.72	3.39	46	2.07	.044	.30	[.10, 6.69]
Aligned	26.61	14.28						
Block 2								
Misaligned	22.53	10.01	2.04	46	1.86	.069	.27	[−.17, 4.26]
Aligned	20.49	9.03						
Block 3								
Misaligned	21.85	7.60	4.42	46	4.81	<.001	.70	[2.57, 6.23]
Aligned	17.43	7.21						
Block 4								
Misaligned	22.59	8.16	4.07	46	3.65	<.001	.53	[1.83, 6.31]
Aligned	18.52	8.61						
Block 5								
Misaligned	22.72	8.07	5.05	46	4.48	<.001	.65	[2.78, 7.33]
Aligned	17.67	8.85						
Block 6								
Misaligned	22.59	8.73	3.96	46	2.97	.005	.43	[1.28, 6.65]
Aligned	18.63	11.47						

Note. *df* = degrees of freedom; CI = confidence interval.

were not significantly different from headings facing South ($M = 25.33$, $SD = 18.20$), $t(39) = -2.13$, $p = .120$, 95% CI [−14.48, −0.36], along the same axis; all p values were Bonferroni corrected for three comparisons on each block (North vs. East, North vs. South, North vs. West). North-facing headings were not significantly different from other imagined cardinal headings on any subsequent testing blocks. Performance for each cardinal facing direction across testing blocks is shown in Figure S7 (in the online supplemental materials). There was no statistical difference between learning on Block 1 in Experiment 2 ($M = 31.19$, $SD = 17.41$) versus Experiment 3 ($M = 28.30$, $SD = 13.56$), $t(26.89) = -1.00$, $p > .250$, 95% CI [−8.82, 2.84].

Additional analyses. As there was no navigation component to Experiment 3, no additional analyses related to excess path or head direction could be conducted.

Discussion

Participants learned maps of a VE, interspersed with JRDs. Alignment effects were detected on the first block when only maps were used for learning. This suggests that route learning, which has been shown to produce slower improvements in JRD relative to maps (Zhang et al., 2014), may interfere with the ability to utilize alignment effects obtained from a map. Participants may prefer the use of a reference frame based on the first learning modality, maps, in Experiment 2, with some degradation in memory for that reference frame related to time spent in navigation. Another possibility is that the use of an initial or salient reference frame during navigation may have interfered with alignment effects but not performance (see Figure S6 in the online supplemental materials), particularly if the "map" and "navigation" reference frames were initially inconsistent (Gagnon et al., 2014), that is, the one selected during navigation was geometrically incorrect because participants were still attempting to encode the shape of boundaries during navigation. This would also be consistent with findings from recent work by Meilinger, Frankenstein, Watanabe, Bülthoff, and Hölscher (2015), which found that participants selected reference frames based on learning order despite utility of the information provided from that learning modality for subsequent memory goals. Interestingly, any interference in reference frame may be specific to the formation of alignment effects here, as absolute pointing error on the first block was not different between Experiments 2 and 3. That is to say, our learning manipulation across experiments on the first block (map, then navigation, before JRD in Experiment 2 versus only map before JRD in Experiment 3) had an effect on whether or not alignment effects were employed but not on overall memory precision on the JRD task.

General Discussion

In Experiment 1, participants freely ambulated in an immersive VR interface using an omnidirectional treadmill to navigate to target landmarks. Then, they performed the JRD task with headings that were either aligned or misaligned with the salient geometry of the environment, repeating this process of navigation and JRD pointing six times total. Based on LGC, Bayes null, and post hoc tests, we found no evidence for differential performance on aligned versus misaligned JRD trials initially. In fact, the LGC results supported a model for Experiment 1, in which the intercept means were the same but the slope means differed for aligned versus misaligned pointing. Thus, Experiment 1 supported the idea that alignment effects are emergent, experience-dependent phenomena in novel environments.

It could be argued, however, that large-scale, real-world environments are rarely learned by direct exploration alone. If participants were aware of the rectangular structure of the surrounding geometry, they might be more likely to show alignment effects, as argued in past work (Frankenstein et al., 2012; Marchette et al., 2011). Additionally, it may have been that we did not observe alignment effects in Experiment 1 because absolute pointing error and variance were high on the first blocks because participants

lacked familiarity with the environment. By preexposing participants to maps in Experiment 2, we thus directly tested whether knowledge of the surrounding spatial geometry via exposure to maps prior to exploration of a novel environment would produce more immediate alignment effects. Despite preexposure to a map before navigating, we still did not find alignment effects initially, again supported by our LGC, Bayes null, and post hoc tests. Specifically, the LGC results again supported a model in which the intercept means were the same but the slope means varied. These findings again support the idea that alignment effects are an experience-dependent, emergent phenomenon in novel environments.

Experiment 3 used the same procedures as Experiment 1 but employed only map learning instead of navigation learning. Somewhat surprisingly, alignment effects were present on the first block, supported by LGC, Bayes null, and post hoc tests. Specifically, LGC results supported the conclusion that, in this case, the model in which the intercept means differed, but not the slope means (total change across learning), was most parsimonious in explaining the findings. Notably, the presence of alignment effects on the first block during map learning was also true for a matched sample size ($N = 24$) using post hoc tests. Overall performance on the first block of Experiment 3 was not different from that of Experiment 2, ruling out the possibility that poor performance could account for the lack of an alignment effect on the first block of Experiment 2.

An important question then regards why we observed alignment effects on the first block of Experiment 3, which involved studying a map, but not until Block 3 in Experiment 2, which involved studying a map and then navigating. There are several possibilities. The interference introduced by route-based information following map learning in Experiment 2 may have been selective to the ability to apply useful geometric-based reference frames to spatial memories formed during navigation but not on the memories more generally, as indicated by the fact that participants did show alignment affects when studying the map only. It could also be that alignment effects are simply more salient in spaces of certain scales, consistent with findings of differences between vista versus environmental spaces (Meilinger et al., 2016). It is also worth noting that maps can be considered a form of configural space (Montello, 1993), given that the actual distances are smaller and that in many situations with maps, such as our map task, all relevant items can be seen from one perspective.

Although the issues of environmental scale and alignment effects have been tested, to some extent, previously by varying display sizes or imagined size of the observer (Presson, DeLange, & Hazelrigg, 1989; Roskos-Ewoldsen, McNamara, Shelton, & Carr, 1998), the specific differences between vista space versus environmental space versus configural space have not been directly addressed using novel environments which participants freely navigate. The difference observed in our study may prove useful in further understanding spatial learning and additional conditions that may directly affect alignment effect formation, and although earlier studies have argued that scale may not have an impact on alignment effects (P. N. Wilson, Tlauka, & Wildbur, 1999), others have emphasized the importance in spatial scale as it relates to the neural mechanisms, neural systems, and cognitive processes engaged in the brain (Ekstrom et al., 2017; Wolbers & Wiener, 2014). Thus, although we cannot be sure why alignment effects emerged during map studying but not route learning, nor during route learning preceded by map learning, overall, our findings are consistent with the idea that spatial representation may differ as a function of scale of space.

Our findings, taken together, provide evidence for situations in which spatial boundaries, as an organizing schema for initial spatial knowledge, are either not yet behaviorally relevant or are suppressed by interfering information. A novel affordance of our VR interface, compared with real-world studies, is the ability to measure behavior between learning exposures and record detailed information about movement, body position, and head direction. This provided us with a sensitive metric of how spatial representations were formed and how they changed over time. Extensive learning of more complex environments, such as the city of Tübingen used by Frankenstein et al. (2012), may provide further insight as to how these representations change as participants become experts of an environment. This and other research posit that map learning may play a critical role in orienting spatial alignments to a geometric reference frame (Richardson, Montello, & Hegarty, 1999). Building on previous studies using pointing error metrics (Zhang et al., 2014), future studies might further examine the effects of various learning conditions (e.g., routes vs. maps) on the emergence of alignment effects and how various reference frames contribute to detecting these effects in more egocentric or allocentric tasks (e.g., Gramann et al., 2010).

Our study used a primarily allocentric pointing task, the JRD, rather than a more egocentric task like the scene- and orientation-dependent pointing task, with the JRD task benefiting more from map learning than route learning (Thorndyke & Hayes-Roth, 1982; Zhang et al., 2014). A remaining question is whether or not route learning is actually beneficial for primarily allocentric spatial memory when a map is available. This would be consistent with findings that suggest humans generally rely on allocentric strategies, unless high-fidelity allocentric information is not available, in which case egocentric reference frames are primarily utilized (Mou, McNamara, Rump, & Xiao, 2006; Newman et al., 2007). Further investigation into the cognitive and neural mechanisms involved in reference frame switching may provide useful insights in addition to electrophysiological and neuroimaging studies of spatial representation formation (Ekstrom, 2010; Ekstrom, Arnold, & Iaria, 2014; Ekstrom et al., 2017; Ishikawa & Montello, 2006).

Studies that have explicitly investigated the dynamics of place-cell firing over repeated exposure to the environment on a single day suggest that neural coding for position does not initially show a strong direction bias but instead emerges based on experience (Ekstrom et al., 2001; Mehta et al., 1997, 2000). These studies, though, were physiological, conducted in rodents, and did not investigate binding to the surrounding geometry of the environment or specific viewpoints (the latter of which would be challenging to address in rats because of their limited vision). Although rodent electrophysiology studies also suggest the importance of spatial boundaries to location-coding mechanisms more generally (Barry et al., 2006; Hartley, Lever, Burgess, & O'Keefe, 2014), our findings shed new light on when we incorporate spatial boundaries into environment-specific representations during navigation. Particularly, our findings add to the spatial navigation literature by suggesting that alignment effects emerge later in novel spatial environments following sufficient exposure, particu-

larly that which allows egocentric to allocentric conversion between the surrounding environment and specific viewpoints and trajectories (Gramann, Müller, Eick, & Schönebeck, 2005; Zhang et al., 2014). To our knowledge, such findings have yet to be shown in rodents, suggesting a potential novel line of research, for example, whether place cells show differences in firing rate as a function of alignment of trajectories to the surrounding spatial geometry. This could also help better inform the factors influencing development of unidirectional versus omnidirectional place cells, a topic of current debate in the field (Buzsáki & Moser, 2013).

One potential consideration when interpreting the results of our navigation-based experiments (Experiments 1 and 2) is the lack of distal landmarks, like mountains. Could these, potentially, have served to more rapidly anchor representations formed during navigation to a primary axis? Despite the absence of distal landmarks, a feature also not included in many small-scale studies showing environmental alignment effects (Kelly et al., 2007; Mou & McNamara, 2002; Mou et al., 2004; Rump & McNamara, 2013; Shelton & McNamara, 2001), participants nonetheless establish a primary reference axis even in the absence of salient, orthogonal, distal landmarks (Han & Becker, 2014). The question of how distal landmarks can be utilized to anchor representations for space or how the same distal landmark may differentially anchor representations for separately represented compartments of adjacent spaces is an important one but is outside the scope of the present work, which followed up on past studies showing that the shape of the spatial boundaries results in environmental alignment effects during the JRD task. Thus, we do not believe that the lack of distal landmarks should limit the interpretation of these findings.

In conclusion, our three experiments highlight the dynamic formation of spatial representations throughout the learning of novel, large-scale, realistic environments involving free ambulation. We demonstrate conditions under which alignment effects are and are not present in initial JRD pointing performance, with these effects emerging after repeated learning, be it from route-learning either in isolation or preceded by map-learning. To be clear, our findings do not refute the presence of alignment effects during navigation of large-scale space, as these were clearly present in later blocks of learning. Rather, the goal of this research was to identify conditions that may lead us to better understand the putative cognitive processes that underlie spatial representation formation and when geometric axes are effectively integrated into those representations for behavioral goals. We also speculate on the potential dynamic effects route and map learning have on one another when both are present early in learning and how this might relate to the issue of scale of space. The findings provide a foundation for the future study of spatial cognition in large-scale, realistic spatial environments using a novel VR interface that provides, to our knowledge, the closest experience to real-world navigation of large-scale, city-sized environments to date. This is because our interface incorporates optic flow, as well as vestibular, proprioceptive, and somatosensory information, and the ability to freely ambulate in large-scale VEs. We thus provide a novel means, and novel data, regarding how spatial representations evolve during learning.

References

Abbott, L. F., & Blum, K. I. (1996). Functional significance of long-term potentiation for sequence learning and prediction. *Cerebral Cortex, 6,* 406–416. http://dx.doi.org/10.1093/cercor/6.3.406

Barry, C., Lever, C., Hayman, R., Hartley, T., Burton, S., O'Keefe, J., . . . Burgess, N. (2006). The boundary vector cell model of place cell firing and spatial memory. *Reviews in the Neurosciences, 17,* 71–97. http://dx.doi.org/10.1515/REVNEURO.2006.17.1-2.71

Buzsáki, G., & Moser, E. I. (2013). Memory, navigation and theta rhythm in the hippocampal-entorhinal system. *Nature Neuroscience, 16,* 130–138. http://dx.doi.org/10.1038/nn.3304

Byrne, P., Becker, S., & Burgess, N. (2007). Remembering the past and imagining the future: A neural model of spatial memory and imagery. *Psychological Review, 114,* 340–375. http://dx.doi.org/10.1037/0033-295X.114.2.340

Chan, E., Baumann, O., Bellgrove, M. A., & Mattingley, J. B. (2013). Reference frames in allocentric representations are invariant across static and active encoding. *Frontiers in Psychology, 4,* 565. http://dx.doi.org/10.3389/fpsyg.2013.00565

Chrastil, E. R., & Warren, W. H. (2012). Active and passive contributions to spatial learning. *Psychonomic Bulletin & Review, 19,* 1–23. http://dx.doi.org/10.3758/s13423-011-0182-x

Chrastil, E. R., & Warren, W. H. (2013). Active and passive spatial learning in human navigation: Acquisition of survey knowledge. *Journal of Experimental Psychology: Learning, Memory, and Cognition, 39,* 1520–1537. http://dx.doi.org/10.1037/a0032382

Chrastil, E. R., & Warren, W. H. (2014). From cognitive maps to cognitive graphs. *PLoS ONE, 9,* e112544. http://dx.doi.org/10.1371/journal.pone.0112544

Cousineau, D. (2005). Confidence intervals in within-subject designs: A simpler solution to Loftus and Masson's method. *Tutorials in Quantitative Methods for Psychology, 1,* 42–45. http://dx.doi.org/10.20982/tqmp.01.1.p042

Crandall, C. S., Preisler, J. J., & Aussprung, J. (1992). Measuring life event stress in the lives of college students: The Undergraduate Stress Questionnaire (USQ). *Journal of Behavioral Medicine, 15,* 627–662. http://dx.doi.org/10.1007/BF00844860

Ekstrom, A. D. (2010). Navigation in Virtual Space: Psychological and Neural Aspects. In G. F. Koob, M. L. Moal, & R. F. Thompson (Eds.), *Encyclopedia of behavioral neuroscience* (Vol. 2, pp. 286–293). London, UK: Academic Press.

Ekstrom, A. D., Arnold, A. E., & Iaria, G. (2014). A critical review of the allocentric spatial representation and its neural underpinnings: Toward a network-based perspective. *Frontiers in Human Neuroscience, 8,* 803. http://dx.doi.org/10.3389/fnhum.2014.00803

Ekstrom, A. D., Huffman, D. J., & Starrett, M. (2017). Interacting networks of brain regions underlie human spatial navigation: A review and novel synthesis of the literature. *Journal of Neurophysiology, 118,* 3328–3344. http://dx.doi.org/10.1152/jn.00531.2017

Ekstrom, A. D., & Isham, E. A. (2017). Human spatial navigation: Representations across dimensions and scales. *Current Opinion in Behavioral Sciences, 17*(Suppl. C), 84–89. http://dx.doi.org/10.1016/j.cobeha.2017.06.005

Ekstrom, A. D., Kahana, M. J., Caplan, J. B., Fields, T. A., Isham, E. A., Newman, E. L., & Fried, I. (2003). Cellular networks underlying human spatial navigation. *Nature, 425,* 184–188. http://dx.doi.org/10.1038/nature01964

Ekstrom, A. D., Meltzer, J., McNaughton, B. L., & Barnes, C. A. (2001). NMDA receptor antagonism blocks experience-dependent expansion of hippocampal "place fields." *Neuron, 31,* 631–638. http://dx.doi.org/10.1016/S0896-6273(01)00401-9

Epstein, R. A. (2008). Parahippocampal and retrosplenial contributions to human spatial navigation. *Trends in Cognitive Sciences, 12,* 388–396. http://dx.doi.org/10.1016/j.tics.2008.07.004

Ferrer, E., Hamagami, F., & McArdle, J. J. (2004). Modeling latent growth curves with incomplete data using different types of structural equation modeling and multilevel software. *Structural Equation Modeling, 11,* 452–483. http://dx.doi.org/10.1207/s15328007sem1103_8

Ferrer, E., & McArdle, J. J. (2003). Alternative structural models for multivariate longitudinal data analysis. *Structural Equation Modeling, 10,* 493–524. http://dx.doi.org/10.1207/S15328007SEM1004_1

Frankenstein, J., Mohler, B. J., Bülthoff, H. H., & Meilinger, T. (2012). Is the map in our head oriented north? *Psychological Science, 23,* 120–125. http://dx.doi.org/10.1177/0956797611429467

Gagnon, S. A., Brunyé, T. T., Gardony, A., Noordzij, M. L., Mahoney, C. R., & Taylor, H. A. (2014). Stepping into a map: Initial heading direction influences spatial memory flexibility. *Cognitive Science, 38,* 275–302. http://dx.doi.org/10.1111/cogs.12055

Gramann, K., Müller, H. J., Eick, E. M., & Schönebeck, B. (2005). Evidence of separable spatial representations in a virtual navigation task. *Journal of Experimental Psychology: Human Perception and Performance, 31,* 1199–1223. http://dx.doi.org/10.1037/0096-1523.31.6.1199

Gramann, K., Onton, J., Riccobon, D., Mueller, H. J., Bardins, S., & Makeig, S. (2010). Human brain dynamics accompanying use of egocentric and allocentric reference frames during navigation. *Journal of Cognitive Neuroscience, 22,* 2836–2849. http://dx.doi.org/10.1162/jocn.2009.21369

Han, X., & Becker, S. (2014). One spatial map or many? Spatial coding of connected environments. *Journal of Experimental Psychology: Learning, Memory, and Cognition, 40,* 511–531. http://dx.doi.org/10.1037/a0035259

Hartley, T., Lever, C., Burgess, N., & O'Keefe, J. (2014). Space in the brain: How the hippocampal formation supports spatial cognition. *Philosophical Transactions of the Royal Society of London*. Series B, Biological Sciences, *369,* 20120510. http://dx.doi.org/10.1098/rstb.2012.0510

Huffman, D. J., & Ekstrom, A. D. (2018). *Which way is the bookstore? A closer look at the judgments of relative direction task*. Manuscript submitted for publication.

Huffman, D. J., & Stark, C. E. L. (2017). The influence of low-level stimulus features on the representation of contexts, items, and their mnemonic associations. *NeuroImage, 155,* 513–529. http://dx.doi.org/10.1016/j.neuroimage.2017.04.019

Huttenlocher, J., Hedges, L. V., Corrigan, B., & Crawford, L. E. (2004). Spatial categories and the estimation of location. *Cognition, 93,* 75–97. http://dx.doi.org/10.1016/j.cognition.2003.10.006

Iachini, T., & Logie, R. H. (2003). The role of perspective in locating position in a real-world, unfamiliar environment. *Applied Cognitive Psychology, 17,* 715–732. http://dx.doi.org/10.1002/acp.904

Ishikawa, T., & Montello, D. R. (2006). Spatial knowledge acquisition from direct experience in the environment: Individual differences in the development of metric knowledge and the integration of separately learned places. *Cognitive Psychology, 52,* 93–129. http://dx.doi.org/10.1016/j.cogpsych.2005.08.003

Jöreskog, K. G. (1971). Simultaneous factor analysis in several populations. *Psychometrika, 36,* 409–426. http://dx.doi.org/10.1007/Bf02291366

Judd, C. M., McClelland, G. H., & Culhane, S. E. (1995). Data analysis: Continuing issues in the everyday analysis of psychological data. *Annual Review of Psychology, 46,* 433–465. http://dx.doi.org/10.1146/annurev.ps.46.020195.002245

Kelly, J. W., Avraamides, M. N., & Loomis, J. M. (2007). Sensorimotor alignment effects in the learning environment and in novel environments. *Journal of Experimental Psychology: Learning, Memory, and Cognition, 33,* 1092–1107. http://dx.doi.org/10.1037/0278-7393.33.6.1092

Kennedy, R. S., Lane, N. E., Berbaum, K. S., & Lilienthal, M. G. (1993). Simulator Sickness Questionnaire: An enhanced method for quantifying simulator sickness. *The International Journal of Aviation Psychology, 3,* 203–220. http://dx.doi.org/10.1207/s15327108ijap0303_3

Marchette, S. A., Yerramsetti, A., Burns, T. J., & Shelton, A. L. (2011). Spatial memory in the real world: Long-term representations of everyday environments. *Memory & Cognition, 39,* 1401–1408. http://dx.doi.org/10.3758/s13421-011-0108-x

Markus, E. J., Qin, Y. L., Leonard, B., Skaggs, W. E., McNaughton, B. L., & Barnes, C. A. (1995). Interactions between location and task affect the spatial and directional firing of hippocampal neurons. *The Journal of Neuroscience, 15,* 7079–7094.

May, M. (2004). Imaginal perspective switches in remembered environments: Transformation versus interference accounts. *Cognitive Psychology, 48,* 163–206. http://dx.doi.org/10.1016/S0010-0285(03)00127-0

McArdle, J. J. (2009). Latent variable modeling of differences and changes with longitudinal data. *Annual Review of Psychology, 60,* 577–605. http://dx.doi.org/10.1146/annurev.psych.60.110707.163612

McNamara, T. P., Rump, B., & Werner, S. (2003). Egocentric and geocentric frames of reference in memory of large-scale space. *Psychonomic Bulletin & Review, 10,* 589–595. http://dx.doi.org/10.3758/BF03196519

McNaughton, B. L., Barnes, C. A., & O'Keefe, J. (1983). The contributions of position, direction, and velocity to single unit activity in the hippocampus of freely-moving rats. *Experimental Brain Research, 52,* 41–49. http://dx.doi.org/10.1007/BF00237147

Mehta, M. R., Barnes, C. A., & McNaughton, B. L. (1997). Experience-dependent, asymmetric expansion of hippocampal place fields. *PNAS Proceedings of the National Academy of Sciences of the United States of America, 94,* 8918–8921. http://dx.doi.org/10.1073/pnas.94.16.8918

Mehta, M. R., Quirk, M. C., & Wilson, M. A. (2000). Experience-dependent asymmetric shape of hippocampal receptive fields. *Neuron, 25,* 707–715. http://dx.doi.org/10.1016/S0896-6273(00)81072-7

Meilinger, T., Frankenstein, J., Watanabe, K., Bülthoff, H. H., & Hölscher, C. (2015). Reference frames in learning from maps and navigation. *Psychological Research, 79,* 1000–1008. http://dx.doi.org/10.1007/s00426-014-0629-6

Meilinger, T., Strickrodt, M., & Bülthoff, H. H. (2016). Qualitative differences in memory for vista and environmental spaces are caused by opaque borders, not movement or successive presentation. *Cognition, 155,* 77–95. http://dx.doi.org/10.1016/j.cognition.2016.06.003

Miller, J. F., Neufang, M., Solway, A., Brandt, A., Trippel, M., Mader, I., . . . Schulze-Bonhage, A. (2013). Neural activity in human hippocampal formation reveals the spatial context of retrieved memories. *Science, 342,* 1111–1114. http://dx.doi.org/10.1126/science.1244056

Moar, I., & Bower, G. H. (1983). Inconsistency in spatial knowledge. *Memory & Cognition, 11,* 107–113. http://dx.doi.org/10.3758/BF03213464

Montello, D. R. (1993). Scale and multiple psychologies of space. In A. U. Frank & I. Campari (Eds.), *Spatial information theory: A theoretical basis for GIS. Proceedings of COSIT '93. Lecture Notes in Computer Science* (Vol. 716, pp. 312–321). Berlin, Germany: Springer-Verlag.

Mou, W., & McNamara, T. P. (2002). Intrinsic frames of reference in spatial memory. *Journal of Experimental Psychology: Learning, Memory, and Cognition, 28,* 162–170. http://dx.doi.org/10.1037/0278-7393.28.1.162

Mou, W., McNamara, T. P., Rump, B., & Xiao, C. (2006). Roles of egocentric and allocentric spatial representations in locomotion and reorientation. *Journal of Experimental Psychology: Learning, Memory, and Cognition, 32,* 1274–1290. http://dx.doi.org/10.1037/0278-7393.32.6.1274

Mou, W., McNamara, T. P., Valiquette, C. M., & Rump, B. (2004). Allocentric and egocentric updating of spatial memories. *Journal of Experimental Psychology: Learning, Memory, and Cognition, 30,* 142–157. http://dx.doi.org/10.1037/0278-7393.30.1.142

Muller, R. U., Bostock, E., Taube, J. S., & Kubie, J. L. (1994). On the directional firing properties of hippocampal place cells. *The Journal of Neuroscience, 14,* 7235–7251.

Muthén, L. K., & Muthén, B. O. (1998–2010). *Mplus user's guide* (6th ed.). Los Angeles, CA: Author.

Newman, E. L., Caplan, J. B., Kirschen, M. P., Korolev, I. O., Sekuler, R., & Kahana, M. J. (2007). Learning your way around town: How virtual taxicab drivers learn to use both layout and landmark information. *Cognition, 104,* 231–253. http://dx.doi.org/10.1016/j.cognition.2006.05.013

O'Keefe, J. (1976). Place units in the hippocampus of the freely moving rat. *Experimental Neurology, 51,* 78–109. http://dx.doi.org/10.1016/0014-4886(76)90055-8

Presson, C. C., DeLange, N., & Hazelrigg, M. D. (1989). Orientation specificity in spatial memory: What makes a path different from a map of the path? *Journal of Experimental Psychology: Learning, Memory, and Cognition, 15,* 887–897. http://dx.doi.org/10.1037/0278-7393.15.5.887

R Development Core Team. (2016). *R: A language and environment for statistical computing*. Vienna, Austria: R Foundation for Statistical Computing. Retrieved from https://www.r-project.org/

Richardson, A. E., Montello, D. R., & Hegarty, M. (1999). Spatial knowledge acquisition from maps and from navigation in real and virtual environments. *Memory & Cognition, 27,* 741–750. http://dx.doi.org/10.3758/BF03211566

Rieser, J. J. (1989). Access to knowledge of spatial structure at novel points of observation. *Journal of Experimental Psychology: Learning, Memory, and Cognition, 15,* 1157–1165. http://dx.doi.org/10.1037/0278-7393.15.6.1157

Roskos-Ewoldsen, B., McNamara, T. P., Shelton, A. L., & Carr, W. (1998). Mental representations of large and small spatial layouts are orientation dependent. *Journal of Experimental Psychology: Learning, Memory, and Cognition, 24,* 215–226. http://dx.doi.org/10.1037/0278-7393.24.1.215

Rouder, J. N., Speckman, P. L., Sun, D., Morey, R. D., & Iverson, G. (2009). Bayesian t tests for accepting and rejecting the null hypothesis. *Psychonomic Bulletin & Review, 16,* 225–237. http://dx.doi.org/10.3758/PBR.16.2.225

RStudio Team. (2015). *RStudio: Integrated development environment for R* (Version 0.99.903). Boston, MA: RStudio, Inc. Retrieved from http://www.rstudio.com/

Ruddle, R. A., & Lessels, S. (2006). For efficient navigational search, humans require full physical movement, but not a rich visual scene. *Psychological Science, 17,* 460–465. http://dx.doi.org/10.1111/j.1467-9280.2006.01728.x

Ruddle, R. A., & Lessels, S. (2009). The benefits of using a walking interface to navigate virtual environments. *ACM Transactions on Computer-Human Interaction, 16,* 1–18. http://dx.doi.org/10.1145/1502800.1502805

Ruddle, R. A., Payne, S. J., & Jones, D. M. (1999). Navigating large-scale virtual environments: What differences occur between helmet-mounted and desk-top displays? *Presence, 8,* 157–168. http://dx.doi.org/10.1162/105474699566143

Rump, B., & McNamara, T. P. (2013). Representations of interobject spatial relations in long-term memory. *Memory & Cognition, 41,* 201–213. http://dx.doi.org/10.3758/s13421-012-0257-6

Shelton, A. L., & Marchette, S. A. (2010). Where do you think you are? Effects of conceptual current position on spatial memory performance. *Journal of Experimental Psychology: Learning, Memory, and Cognition, 36,* 686–698. http://dx.doi.org/10.1037/a0018713

Shelton, A. L., & McNamara, T. P. (2001). Systems of spatial reference in human memory. *Cognitive Psychology, 43,* 274–310. http://dx.doi.org/10.1006/cogp.2001.0758

Stevens, A., & Coupe, P. (1978). Distortions in judged spatial relations. *Cognitive Psychology, 10,* 422–437. http://dx.doi.org/10.1016/0010-0285(78)90006-3

Taube, J. S., Valerio, S., & Yoder, R. M. (2013). Is navigation in virtual reality with FMRI really navigation? *Journal of Cognitive Neuroscience, 25,* 1008–1019. http://dx.doi.org/10.1162/jocn_a_00386

Thorndyke, P. W., & Hayes-Roth, B. (1982). Differences in spatial knowledge acquired from maps and navigation. *Cognitive Psychology, 14,* 560–589. http://dx.doi.org/10.1016/0010-0285(82)90019-6

Waller, D., Hunt, E., & Knapp, D. (1998). The transfer of spatial knowledge in virtual environment training. *Presence, 7,* 129–143. http://dx.doi.org/10.1162/105474698565631

Waller, D., Montello, D. R., Richardson, A. E., & Hegarty, M. (2002). Orientation specificity and spatial updating of memories for layouts. *Journal of Experimental Psychology: Learning, Memory, and Cognition, 28,* 1051–1063. http://dx.doi.org/10.1037/0278-7393.28.6.1051

Wang, R. F. (2017). Spatial updating and common misinterpretations of spatial reference frames. *Spatial Cognition and Computation, 17,* 222–249. http://dx.doi.org/10.1080/13875868.2017.1304394

Werner, S., & Schmidt, K. (1999). Environmental reference systems for large-scale spaces. *Spatial Cognition and Computation, 1,* 447–473. http://dx.doi.org/10.1023/A:1010095831166

West, S. G., Taylor, A. B., & Wu, W. (2012). Model fit and model selection in structural equation modeling. In R. H. Hoyle (Ed.), *Handbook of structural equation modeling* (pp. 209–231). New York, NY: Guilford Press.

Wilson, M. A., & McNaughton, B. L. (1993). Dynamics of the hippocampal ensemble code for space. *Science, 261,* 1055–1058. http://dx.doi.org/10.1126/science.8351520

Wilson, P. N., Tlauka, M., & Wildbur, D. (1999). Orientation specificity occurs in both small- and large-scale imagined routes presented as verbal descriptions. *Journal of Experimental Psychology: Learning, Memory, and Cognition, 25,* 664–679. http://dx.doi.org/10.1037/0278-7393.25.3.664

Wolbers, T., & Wiener, J. M. (2014). Challenges for identifying the neural mechanisms that support spatial navigation: The impact of spatial scale. *Frontiers in Human Neuroscience, 8,* 571. http://dx.doi.org/10.3389/fnhum.2014.00571

Zhang, H., & Ekstrom, A. (2013). Human neural systems underlying rigid and flexible forms of allocentric spatial representation. *Human Brain Mapping, 34,* 1070–1087. http://dx.doi.org/10.1002/hbm.21494

Zhang, H., Zherdeva, K., & Ekstrom, A. D. (2014). Different "routes" to a cognitive map: Dissociable forms of spatial knowledge derived from route and cartographic map learning. *Memory & Cognition, 42,* 1106–1117. http://dx.doi.org/10.3758/s13421-014-0418-x

Received November 6, 2017
Revision received January 19, 2018
Accepted February 25, 2018 ■